EUROPEAN ORGANIZATION FOR NUCLEAR RESEARCH

CERN-EP/98-45
June 4, 1998

Measurement of the anomalous magnetic and electric dipole moments of the tau lepton

The L3 Collaboration

Abstract

We analyse $e^+e^- \to \tau\tau\gamma$ events using $100\,\mathrm{pb}^{-1}$ of data collected by the L3 experiment during the 1991-1995 LEP runs at the Z pole. From the energy of the photons and their isolation from the tau decay products, we determine the anomalous magnetic and electric dipole moments of the tau to be, respectively:

$$\begin{aligned} a_\tau &= 0.004 \pm 0.027 \pm 0.023; \\ d_\tau &= (0.0 \pm 1.5 \pm 1.3) \times 10^{-16} e\cdot\mathrm{cm}. \end{aligned}$$

This is a direct measurement of these τ form factors at $q^2 = 0$.

Submitted to *Phys. Lett. B*

Introduction

In the Standard Model (SM), the electromagnetic interactions of each of the three charged leptons are identical. There is, however, no experimentally verified explanation for why there are three generations of leptons nor for why they have such differing masses. New insight might be forthcoming if the leptons were observed to have substructure, which could manifest itself in deviations from the SM values for the anomalous magnetic or electric dipole moments. The anomalous moments for the electron and muon have been measured with very high precision [1] compared to those of tau for which there are only upper limits [2–4].

In general a photon may couple to a tau through its electric charge, magnetic dipole moment, or electric dipole moment. This coupling may be parametrised using a matrix element in which the usual γ^μ is replaced by a more general Lorentz-invariant form,

$$\Gamma^\mu = F_1(q^2)\gamma^\mu + F_2(q^2)\frac{i}{2m_\ell}\sigma^{\mu\nu}q_\nu - F_3(q^2)\sigma^{\mu\nu}\gamma^5 q_\nu. \tag{1}$$

The q^2-dependent form-factors[1)] , $F_i(q^2)$, have familiar interpretations for $q^2 = 0$: $F_1(0) \equiv Q_\tau$ is the electric charge; $F_2(0) \equiv a_\tau$ is the anomalous magnetic moment ($a_\tau \equiv (g_\tau - 2)/2$); and $F_3(0) \equiv d_\tau/Q_\tau$, where d_τ is the electric dipole moment. In the SM a_τ is non-zero due to loop diagrams and is predicted to be $a_\tau^{\mathrm{SM}} = 0.001\,177\,3(3)$ [5,6]. A non-zero value of d_τ is forbidden by both P invariance and T invariance. Assuming CPT invariance, observation of a non-zero value of d_τ would imply CP violation.

The process $\mathrm{e^+e^-} \to \gamma \to \tau^+\tau^-$ has been used to constrain F_2 and F_3 at q^2 up to $(37\ \mathrm{GeV})^2$ [2], and an indirect limit has been inferred from the width $\Gamma(Z \to \tau^+\tau^-)$ [3]. The $\mathrm{e^+e^-} \to \tau^+\tau^-\gamma$ cross section has also been used to bound F_2 and F_3 [4]. Only this last method corresponds to a direct measurement at $q^2 = 0$.

In this article, we analyse data collected by the L3 detector [7] at LEP during the period 1991–1995. These data correspond to an integrated luminosity of $100\,\mathrm{pb}^{-1}$ with centre-of-mass energies no more than 400 MeV from the Z pole.

Anomalous electromagnetic moments would enhance the production of high energy isolated photons in $\mathrm{e^+e^-} \to \tau^+\tau^-\gamma$ events, compared to the SM initial and final state radiation processes [8–10]. We therefore select such events and determine the anomalous moments from fits to the distributions of the photon energy and isolation angle, allowing for the SM backgrounds.

Selection of $\mathrm{e^+e^-} \to \tau^+\tau^-(\gamma)$ events

We first select $\mathrm{e^+e^-} \to \tau^+\tau^-(\gamma)$ events and then identify isolated photon candidates. In order to study the various selection criteria and the backgrounds, we use Monte Carlo samples of hadronic events from the JETSET Monte Carlo program [11], two-photon events from DIAG36 [12], Bhabha events from BHAGENE [13], and $\mu\mu(\gamma)$ and $\tau\tau(\gamma)$ events from KORALZ [14]. All Monte Carlo events are passed through the GEANT-based L3 detector simulation program [15], and reconstructed using the same algorithms as for the data.

The selection is confined to the barrel region of the bismuth germanate (BGO) electromagnetic calorimeter, by requiring the event thrust axis be within $|\cos\theta| < 0.74$ where θ is the polar angle with respect to the incoming $\mathrm{e^-}$ beam. Hadronic events are rejected by requiring low multiplicities of charged particle tracks and calorimetric energy clusters. Two-photon events

[1)] Strictly speaking, the F_i are functions of three variables, $F_i(q^2, m_1^2, m_2^2)$, where m_1 and m_2 are the τ masses on either side of the $\tau\tau\gamma$ vertex. In this analysis, $q^2 = 0$, $m_1^2 = m_\tau^2$, and m_2^2, which corresponds to the off-shell τ, is not fixed.

are rejected by requiring that the event contains a total measured energy of more than $0.2\sqrt{s}$ and at least two jets with energies of more than $0.02\sqrt{s}$, where a jet may in some cases consist of a single particle. Cosmic ray muons are rejected by requiring that scintillator hits are in-time with the beam crossing and that charged particle tracks point to the interaction region.

The total energy in the BGO is required to be less than 70 GeV. This cut efficiently removes both non-radiative and radiative Bhabha events, even if showers in the BGO deposit some of their energy in the hadron calorimeter (HCAL). Events in which one electron or photon does not deposit any energy in the BGO, for example because it passes through the material between the crystals, are mostly rejected by requiring that there is no reconstructed electron in the event with an energy exceeding 40 GeV. A reconstructed electron consists of a track pointing to an energy cluster in the BGO, whose lateral shape is consistent with the characteristically narrow profile of an electromagnetic shower. After these cuts, most of the remaining $\mathrm{e^+e^-}\gamma$ background consists of events in which a particle passes down the beam pipe or through the gap between the BGO barrel and endcap modules. To reject this background we require that the missing energy vector of the event, computed using only BGO energy clusters, points into the BGO barrel region.

To remove the $\mathrm{e^+e^-} \to \mu^+\mu^-(\gamma)$ background, all events with two reconstructed muons are rejected. Events with a single muon are rejected if the muon has a momentum of more than 35 GeV(25 GeV) for muons with hits in three(two) of the three layers of the muon chambers.

After applying these selection criteria, we determine the $\mathrm{e^+e^-} \to \tau^+\tau^-(\gamma)$ cross-section at $\sqrt{s} \approx m_\mathrm{Z}$ to be $\sigma_{\tau\tau} = (1.472 \pm 0.006 \pm 0.020)\,\mathrm{nb}$, where the first error is statistical and the second is systematic. The systematic error includes the effects of variations in the selection criteria, the statistics of the Monte Carlo and cosmic ray event samples, and the uncertainties on the subdetector efficiencies, the tau branching fractions, the integrated luminosity, and the trigger efficiency. This is in agreement with the SM prediction of ZFITTER [16] of 1.479 nb, as well as the dedicated L3 lineshape measurement [17], indicating the absence of significant systematic effects in the selection of taus.

Selection of photons in $\mathrm{e^+e^-} \to \tau^+\tau^-(\gamma)$ events

After application of the cuts described above, we next select events with photon candidates in the BGO barrel. A photon candidate comprises an energy cluster in the BGO with a narrow lateral profile and no track within 160 mrad. The background consists of genuine photons from π^0's produced in tau decays, fake photons from mis-identified τ decay products, photon radiation from tau decay products, and a small contribution from Bhabha and dimuon events. Compared to the contribution due to anomalous dipole moments, background photon candidates typically have lower energies, are less isolated from the decay products of the closer tau, and are back-to-back with the decay products of the farther tau. Therefore, we require photon candidates to satisfy $E_\gamma > 3\,\mathrm{GeV}$ and $(0.3 < \psi_\gamma < \pi - 0.3)\,\mathrm{rad}$, where E_γ is the energy of the photon candidate and ψ_γ is the angle between it and the closest calorimetric cluster with energy greater than 1 GeV or 10 GeV for BGO or HCAL clusters respectively. The minimum energy requirements on the closest cluster are chosen to be significantly higher than the expectations for a minimum-ionising muon in order to reduce the residual $\mathrm{e^+e^-} \to \mu^+\mu^-(\gamma)$ background. As discussed below, we have no model for multiple hard radiation including the effects of anomalous dipole moments. Therefore we reject events with more than one photon candidate passing all these selection criteria. Such events constitute about 3% of the sample.

Photon selection efficiency

The simulation and reconstruction of photons in the BGO allows for time-dependent inefficiencies and noise, the characteristics of which are determined on a crystal-by-crystal basis from both online and offline monitoring of the BGO performance. Ultimately, the photon reconstruction efficiency is verified using a sample of $e^+e^- \to \mu^+\mu^-\gamma$ events. Since the muon chamber efficiency is determined using predominantly non-radiative dimuon events, the $\mu\mu\gamma$ sample is sensitive to the photon reconstruction efficiency with little systematic uncertainty from the muon reconstruction efficiency. To select this sample, we first reject non-leptonic events as for the $\tau\tau(\gamma)$ selection and then require that the event contains at least one muon with a momentum of more than 35 GeV. Photons are then selected using the same cuts as for the $\tau\tau\gamma$ selection, with the exception of cuts on the isolation from the closest calorimetric cluster, which are inappropriate for the $\mu\mu\gamma$ environment. To reduce the $\tau\tau\gamma$ background we make a similar but less stringent requirement on the hemisphere opposite the photon of $\psi_{\mu\gamma} < (\pi - 0.15)$ rad, where $\psi_{\mu\gamma}$ is the angle between the photon and the closest muon. Muons leave only a minimum-ionising energy deposit in the BGO of typically 0.25 GeV. Therefore, to retain statistics, no minimum requirement is imposed on $\psi_{\mu\gamma}$. The resulting sample is dominated by genuine $\mu\mu\gamma$ events (99.0%) with only a small contribution from $\tau\tau\gamma$ events (1.0%).

Figure 1 shows the distributions of photon energy E_γ and the isolation angle $\psi_{\mu\gamma}$ of the photon to the closest muon in the selected $\mu\mu\gamma$ event sample. The data are in good agreement with the Monte Carlo prediction. The ratio of the number of photons in data to the number in the Monte Carlo is $0.993 \pm 0.013 \pm 0.003$, where the first error is statistical. The second error is systematic and reflects variations in the photon selection criteria. The shapes of the energy and isolation distributions also agree well, with a chisquare per degree of freedom, based only on the statistical error, of 50.2/44 for the former and 37.6/30 for the latter. This study demonstrates that there are no significant systematic effects in the photon reconstruction.

Modelling of backgrounds

The excellent agreement between data and Monte Carlo for the energy and angular distributions of photons in the $\mu\mu\gamma$ event sample verifies that KORALZ accurately models the radiative dimuon background.

The BHAGENE modelling of photon radiation is checked by selecting radiative Bhabha events. Photons are reconstructed with the same cuts as for the $e^+e^- \to \tau^+\tau^-\gamma$ sample. The shapes of the energy and angular distributions of photons in data and Monte Carlo are found to be in good agreement. A small discrepancy in the total number of radiative Bhabha events predicted by BHAGENE is corrected by weighting such events in the MC so as to agree with the data.

The small background from Bhabhas in the $\tau\tau\gamma$ sample contains events in which an electron passes through the material between the BGO crystals. The simulation of these effects is checked by selecting a sample of events from data with a single well-reconstructed electron of approximately 45 GeV. The magnitude and depth of the BGO and HCAL energy deposits on the opposite side of the event are then compared for data and Monte Carlo, allowing for the small background of non-Bhabha events. It is found that the Monte Carlo simulation of the detector slightly underestimates the number of events with shower leakage or an electron that passes between crystals. Therefore, the Bhabha background events in the final $\tau\tau\gamma$ sample are reweighted as a function of the HCAL energy, if any, of each reconstructed energy cluster.

After applying the $\tau\tau\gamma$ selection criteria and the Bhabha weights described above, 1559 events remain in the data, which is consistent with the SM expectation of 1590 events. The dominant contribution to the $\tau\tau\gamma$ sample is from initial and final state radiation in $e^+e^- \rightarrow \tau^+\tau^-\gamma$ events, with small contributions from Bhabha events (2.3%), di-muon events (2.1%), misidentified tau decay products (1.0%). Contributions from other background sources are negligible.

Determination of a_τ and d_τ

To model the effects of anomalous dipole moments, we use the TTG event generator program [9, 10] which calculates the matrix element, $\mathcal{M}(a_\tau, d_\tau)$, for the process $e^+e^- \rightarrow \tau^+\tau^-\gamma$ allowing for $\mathcal{O}(\alpha)$ SM initial state radiation, final state radiation with both SM and anomalous contributions, both photon and Z exchange, and all interference terms. The TTG calculation of $\mathcal{M}(0,0)$ is checked by comparison with the $O(\alpha)$ predictions of KORALZ. The shapes of the photon energy and angular distributions are in excellent agreement and the overall normalisation agrees to 0.1%. To check the calculation of anomalous effects we compare $\Delta\mathcal{M}^2 = |\mathcal{M}(a_\tau, d_\tau)|^2 - |\mathcal{M}(0,0)|^2$ from TTG to an approximate analytical calculation of $\Delta\mathcal{M}^2$ [8] using the same approximations in TTG as used in the analytical calculation. The anomalous contribution to the cross section agrees to better than 1% [9] and the shapes of the photon energy spectra are in good agreement for a wide range of a_τ and d_τ values.

To allow for detector and reconstruction effects we begin with the fully simulated KORALZ $e^+e^- \rightarrow \tau^+\tau^-\gamma$ event sample which includes initial and final state bremsstrahlung corrections to $O(\alpha^2)$ including exclusive exponentiation. TTG is then used to determine a weight for each KORALZ event which depends on the generated four-vectors of the taus and the photon and on the values of a_τ and d_τ under consideration. Since TTG is an $O(\alpha)$ calculation, there is no unambiguous way to compute a weight for events with more than one photon. We therefore count the number of generator photons with an energy of more than 2.5 GeV and a polar angle θ_γ satisfying $|\cos\theta_\gamma| < 0.8$, where these requirements are looser than those on the corresponding reconstructed quantities in order to allow for the effects of the detector resolution. Then, if the event contains no such photons the weight is set to unity. If the event contains exactly one such photon then the weight is given by the ratio $|\mathcal{M}(a_\tau, d_\tau)|^2/|\mathcal{M}(0,0)|^2$ where $\mathcal{M}$ is the matrix element from TTG. If the event contains more than one photon the weight is set to unity. The effects of this approximation for multiple photon events is treated as a systematic error.

In general, anomalous values of a_τ and d_τ tend to increase the cross section for the process $e^+e^- \rightarrow \tau^+\tau^-\gamma$, especially for photons with high energy which are well isolated from the decay products of the taus. Therefore we use both the total rate and the energy and angular distributions to determine the anomalous moments. The SM Monte Carlo samples are normalised to the measured luminosity. There are a number of kinematic quantities which have varying degrees of sensitivity to a_τ and d_τ, such as the energy and polar angles of the photon and the reconstructed tau decay products, the angle of the photon to one of the taus, or the angle between the two taus. The reconstructed photon energy E_γ and the isolation angle ψ_γ are found to have higher sensitivity and a lower degree of correlation than other pairs of variables.

To determine a_τ and d_τ, binned maximum likelihood fits are made to the two-dimensional distribution of E_γ *vs.* ψ_γ, assuming that the number of data events follows a Poisson distribution. When fitting for a_τ we conservatively set d_τ to the SM value, and *vice versa*. To check the fit method we replace the data with Monte Carlo samples simulating various different values of a_τ and d_τ. The likelihoods for these samples are consistent with the input values of a_τ and d_τ. Since the cross section depends quadratically on the anomalous moments, the likelihood may have two local maxima. We therefore quote the central value (μ) and errors (σ) for a_τ

according to:

$$\int_{-\infty}^{L} \mathcal{L}(a_\tau) da_\tau = \int_{R}^{\infty} \mathcal{L}(a_\tau) da_\tau = 1 - \mathrm{CL}/2; \quad (2)$$

$$\sigma = (R - L)/2; \quad (3)$$

$$\mu = (R + L)/2; \quad (4)$$

where $\mathcal{L}$ is the likelihood function and CL is the desired confidence interval. Similar expressions are used for d_τ.

Figure 2 shows the distributions of E_γ and ψ_γ for the data and the SM Monte Carlo expectation. No excess is apparent at high values as would be expected for significant deviations of a_τ and d_τ from their SM values. The results of the fits to the data, considering only statistical errors, are $a_\tau = 0.004 \pm 0.027$, $d_\tau = (0.0 \pm 1.5) \times 10^{-16} e \cdot \mathrm{cm}$. where the errors refer to the 68.3% confidence interval. These two results are not independent, although the absence of interference terms for d_τ does provide some distinguishing power between the effects of a_τ and those of d_τ [9].

Systematic Errors

The systematic errors include contributions from a number of sources as described below in order of decreasing importance. The quoted errors correspond to the a_τ measurement; errors for d_τ are similar.

- **Event selection cuts**

To estimate the systematic error associated with the choice of selection cuts, all cuts associated with background rejection and photon selection are moved above and below their nominal values, and the resulting distributions are fitted. Wide variations in the cuts associated with Bhabha and dimuon background rejection have little effect, while variation of photon selection cuts, in particular those associated with the photon shower profile and the BGO energy of the cluster nearest the photon, produce the largest effects on the fit result. These sources contribute 0.013 to the fit error.

- **Normalisation of the $\tau\tau(\gamma)$ sample**

We take the combined statistical and systematic error of 1.4% on $\sigma_{\tau\tau}$ to be the uncertainty on the normalisation of the $\tau\tau\gamma$ event sample, due to the $\tau\tau(\gamma)$ selection procedure. This contributes 0.011 to the error.

- **Photon reconstruction**

We take the uncertainty on the photon reconstruction efficiency to be 1.3% as determined from the study of the $\mathrm{e^+e^-} \to \mu^+\mu^-\gamma$ event sample. This is conservative since some effects are covered by the variation of the selection cuts, and contributes 0.010 to the error.

- **Backgrounds**

To determine the uncertainty in the fit from the Monte Carlo statistics of the Bhabha and dimuon background samples, these backgrounds are reduced by their statistical error, this being the conservative direction. This contributes 0.009 to the error. The fit results are insensitive to variations of the Bhabha background within the statistical errors of the $\mathrm{e^+e^-} \to \mathrm{e^+e^-}(\gamma)$ and $\mathrm{e^+e^-} \to \mathrm{e^+e^-}\gamma$ samples used to verify the reweighting corrections for the BHAGENE radiative cross-section and the amount of leakage of electrons into the HCAL. Wide variations in values of the cut variables designed to remove backgrounds other than Bhabhas have a negligible effect on the results.

- **Binning**

The selected sample has been fitted using a variety of binning schemes, all of which include at least 2 bins in E_γ and 2 bins in ψ_γ. The RMS of the errors for this sample is used to assign the systematic error due to binning, which amounts to 0.008.

- **Photon energy scale and resolution**

The BGO energy scale and resolution is determined using *in-situ* calibration systems and by comparison of the BGO energies of electrons in $\mathrm{e^+e^-} \rightarrow \mathrm{e^+e^-}(\gamma)$, $\mathrm{e^+e^-} \rightarrow \tau^+\tau^-(\gamma)$, and $\mathrm{e^+e^-e^+e^-}$ events to the momentum of the corresponding charged track. The invariant mass spectra of pairs of photons from π^0 decays and pairs of electrons from J decays provide additional constraints. The photon energy scale uncertainty is estimated to be less than 0.5% for $E_\gamma \approx 3\,\mathrm{GeV}$ and less than 0.05% for $E_\gamma \approx m_\mathrm{Z}/2$. The BGO energy resolution is estimated to be $(1.7 \pm 0.3\%)$ at $E_\gamma \approx 10\,\mathrm{GeV}$ from the width of the J invariant mass distribution and to be $(1.4 \pm 0.1)\%$ for $E_\gamma \approx m_\mathrm{Z}/2$. The effects of these uncertainties on a_τ and d_τ are determined by varying them, as a function of energy, within their errors, resulting in a contribution to the fit error of 0.008.

- **Modelling of the process** $\mathrm{e^+e^-} \rightarrow \tau^+\tau^-\gamma$

The inclusion of the $\mu\mu\gamma$ normalisation error as a systematic error in the photon reconstruction efficiency allows for possible systematic uncertainties in the KORALZ description of SM photon radiation. The TTG calculation of $\mathcal{M}(0,0)$ agrees with the $O(\alpha)$ predictions of KORALZ to within 0.1%. The TTG calculation of $|\mathcal{M}(a_\tau, d_\tau)|^2$ agrees, for the same approximations, with the analytical calculation [8] to better than 1% [9]. Variation of the TTG predictions within these uncertainties causes a negligible change in the fit results.

- **Multiple photon radiation**

As previously discussed, the weighting procedure used to simulate the effects of anomalous moments affects only the weights of events with a single hard photon. To estimate the effects of neglecting multiple photon radiation, KORALZ is used to generate a sample of $\mathrm{e^+e^-} \rightarrow \tau^+\tau^-(n\gamma)$ events. Then all photons, except for the one with the highest momentum transverse to the closer tau, are incorporated into the four-vectors of the other particles in such a way that all particles remain on mass shell [10]. Weights for various a_τ and d_τ are then computed by TTG using the modified four-vectors of the taus and the photon. Taking these weights in lieu of those computed using the previously described method, in which only events with a single hard photon are considered, has a negligible effect on the result of the fit.

Results

The systematic errors described above are combined, assuming the different sources are uncorrelated, to yield the likelihoods shown in Figure 3. In the case of a_τ, interference between SM and anomalous amplitudes leads to an asymmetric likelihood, while for d_τ the absence of interference at $\mathcal{O}(\alpha)$ leads to a symmetric likelihood. The results are,

$$a_\tau = 0.004 \pm 0.027 \pm 0.023 \quad (5)$$
$$d_\tau = (0.0 \pm 1.5 \pm 1.3) \times 10^{-16} e \cdot \mathrm{cm} \quad (6)$$

where the first error is statistical and the second error is systematic. We also determine limits, including both the statistical and the systematic errors, of $-0.052 < a_\tau < 0.058$ and $(-3.1 < d_\tau < 3.1) \times 10^{-16} e \cdot \mathrm{cm}$ at the 95% confidence level. These results are consistent with SM expectations and improve on the previous upper limits [4].

Acknowledgements

We would like to thank Z. Wąs for his help in the evaluation of the effects of multiple photon radiation. We wish to express our gratitude to the CERN accelerator division for the excellent performance of the LEP machine. We acknowledge with appreciation the effort of all engineers, technicians and support staff who have participated in the construction and maintenance of this experiment.

References

[1] E. R. Cohen and B. N. Taylor, Rev. Mod. Phys. **59** (1987) 1121.

[2] D. J. Silverman and G. L. Shaw, Phys. Rev. **D27** (1983) 1196.

[3] R. Escribano and E. Massó, Phys. Lett. **B395** (1997) 369.

[4] J. A. Grifols and A. Méndez, Phys. Lett. **B 255** (1991) 611, Erratum *ibid* **B259** (1991) 512;
OPAL Collab., CERN-EP/98-033 (Submitted to Phys. Lett. B).

[5] M. A. Samuel, G. Li and R. Mendel, Phys. Rev. Lett. **67** (1991) 668, Erratum *ibid* 69 (1992) 995.

[6] F. Hamzeh and N.F. Nasrallah, Phys. Lett. **B373** (1996) 211.

[7] L3 Collab., B. Adeva *et al.*, Nucl. Instr. & Meth. **A 289** (1990) 35;
M. Acciarri *et al.*, Nucl. Instr. & Meth. **A 351** (1994) 300;
M. Chemarin *et al.*, Nucl. Instr. & Meth. **A 349** (1994) 345;
A. Adam *et al.*, Nucl. Instr. & Meth. **A 383** (1996) 342;
I.C. Brock *et al.*, Nucl. Instr. & Meth. **A 381** (1996) 236.

[8] J. Biebel and T. Riemann, Z. Phys. **C76** (1997) 53.

[9] S.S. Gau, T. Paul, J. Swain, and L. Taylor, HEP-PH/9712360 (to appear in Nucl. Phys. B).

[10] T. Paul and Z. Wąs, HEP-PH/9801301.

[11] T. Sjöstrand, Comp. Phys. Comm. **39** (1986) 347;
T. Sjöstrand and M. Bengtsson, Comp. Phys. Comm. **43** (1987) 367.

[12] F.A. Berends, P.H. Daverveldt and R. Kleiss, Comp. Phys. Comm. **40** (1986) 285.

[13] J. H. Field, Phys. Lett. **B 323** (1994) 432;
J. H. Field and T. Riemann, Comp. Phys. Comm. **94** (1996) 53.

[14] S. Jadach, B. F. L. Ward and Z. Wąs, Comp. Phys. Comm. **79** (1994) 503, KORALZ uses TAUOLA to decay the taus (see: S. Jadach, J.H. Kühn and Z. Wąs, Comp. Phys. Comm. **64** (1991) 275) and PHOTOS for multiple photon radiation (see: E. Barberio, B. van Eijk and Z. Wąs, Comp. Phys. Comm. **66** (1991) 128).

[15] The L3 detector simulation program is based on GEANT Version 3.15 (see: R. Brun *et al.*, "GEANT 3", CERN DD/EE/84-1 revised, (1987)). GHEISHA is used to simulate hadronic interactions (see: H. Fesefeldt, RWTH Aachen Report PITHA 85/02 (1985)). This program allows for the effects of energy loss, multiple scattering, decays and interactions in the detector material, as well as for time-dependent detector effects.

[16] D. Bardin *et al.*, FORTRAN package ZFITTER, and preprint CERN–TH. 6443/92;
D. Bardin *et al.*, Z. Phys. **C 44** (1989) 493;
D. Bardin *et al.*, Nucl. Phys. **B 351** (1991) 1;
D. Bardin *et al.*, Phys. Lett. **B 255** (1991) 290.

[17] L3 Collab., paper in preparation.

The L3 Collaboration:

M.Acciarri,[27] O.Adriani,[16] M.Aguilar-Benitez,[26] S.Ahlen,[11] J.Alcaraz,[26] G.Alemanni,[22] J.Allaby,[17] A.Aloisio,[29] M.G.Alviggi,[29] G.Ambrosi,[19] H.Anderhub,[48] V.P.Andreev,[37] T.Angelescu,[13] F.Anselmo,[9] A.Arefiev,[28] T.Azemoon,[3] T.Aziz,[10] P.Bagnaia,[36] L.Baksay,[43] R.C.Ball,[3] S.Banerjee,[10] Sw.Banerjee,[10] K.Banicz,[45] A.Barczyk,[48,46] R.Barillère,[17] L.Barone,[36] P.Bartalini,[22] A.Baschirotto,[27] M.Basile,[9] R.Battiston,[33] A.Bay,[22] F.Becattini,[16] U.Becker,[15] F.Behner,[48] J.Berdugo,[26] P.Berges,[15] B.Bertucci,[33] B.L.Betev,[48] S.Bhattacharya,[10] M.Biasini,[33] A.Biland,[48] G.M.Bilei,[33] J.J.Blaising,[4] S.C.Blyth,[34] G.J.Bobbink,[2] R.Bock,[1] A.Böhm,[1] L.Boldizsar,[14] B.Borgia,[17,36] D.Bourilkov,[48] M.Bourquin,[19] D.Boutigny,[4] S.Braccini,[19] J.G.Branson,[39] V.Brigljevic,[48] I.C.Brock,[34] A.Buffini,[16] A.Buijs,[44] J.D.Burger,[15] W.J.Burger,[33] J.Busenitz,[43] X.D.Cai,[15] M.Campanelli,[48] M.Capell,[15] G.Cara Romeo,[9] G.Carlino,[29] A.M.Cartacci,[16] J.Casaus,[26] G.Castellini,[16] F.Cavallari,[36] N.Cavallo,[29] C.Cecchi,[19] M.Cerrada,[26] F.Cesaroni,[23] M.Chamizo,[26] Y.H.Chang,[50] U.K.Chaturvedi,[18] S.V.Chekanov,[31] M.Chemarin,[25] A.Chen,[50] G.Chen,[7] G.M.Chen,[7] H.F.Chen,[20] H.S.Chen,[7] M.Chen,[15] G.Chiefari,[29] C.Y.Chien,[5] L.Cifarelli,[38] F.Cindolo,[9] C.Civinini,[16] I.Clare,[15] R.Clare,[15] G.Coignet,[4] A.P.Colijn,[2] N.Colino,[26] S.Costantini,[8] F.Cotorobai,[13] B.de la Cruz,[26] A.Csilling,[14] T.S.Dai,[15] R.D'Alessandro,[16] R.de Asmundis,[29] A.Degré,[4] K.Deiters,[46] P.Denes,[35] F.DeNotaristefani,[36] M.Diemoz,[36] D.van Dierendonck,[2] F.Di Lodovico,[48] C.Dionisi,[17,36] M.Dittmar,[48] A.Dominguez,[39] A.Doria,[29] M.T.Dova,[18,♯] E.Drago,[29] D.Duchesneau,[4] P.Duinker,[2] I.Duran,[40] S.Easo,[33] H.El Mamouni,[25] A.Engler,[34] F.J.Eppling,[15] F.C.Erné,[2] J.P.Ernenwein,[25] P.Extermann,[19] M.Fabre,[46] R.Faccini,[36] M.A.Falagan,[26] S.Falciano,[36] A.Favara,[16] J.Fay,[25] O.Fedin,[37] M.Felcini,[48] T.Ferguson,[34] F.Ferroni,[36] H.Fesefeldt,[1] E.Fiandrini,[33] J.H.Field,[19] F.Filthaut,[17] P.H.Fisher,[15] I.Fisk,[39] G.Forconi,[15] L.Fredj,[19] K.Freudenreich,[48] C.Furetta,[27] Yu.Galaktionov,[28,15] S.N.Ganguli,[10] P.Garcia-Abia,[6] M.Gataullin,[32] S.S.Gau,[12] S.Gentile,[36] J.Gerald,[5] N.Gheordanescu,[13] S.Giagu,[36] S.Goldfarb,[22] J.Goldstein,[11] Z.F.Gong,[20] A.Gougas,[5] G.Gratta,[32] M.W.Gruenewald,[8] R.van Gulik,[2] V.K.Gupta,[35] A.Gurtu,[10] L.J.Gutay,[45] D.Haas,[6] B.Hartmann,[1] A.Hasan,[30] D.Hatzifotiadou,[9] T.Hebbeker,[8] A.Hervé,[17] P.Hidas,[14] J.Hirschfelder,[34] W.C.van Hoek,[31] H.Hofer,[48] H.Hoorani,[34] S.R.Hou,[50] G.Hu,[5] I.Iashvili,[47] B.N.Jin,[7] L.W.Jones,[3] P.de Jong,[17] I.Josa-Mutuberria,[26] A.Kasser,[22] R.A.Khan,[18] D.Kamrad,[47] J.S.Kapustinsky,[24] Y.Karyotakis,[4] M.Kaur,[18,◇] M.N.Kienzle-Focacci,[19] D.Kim,[36] D.H.Kim,[42] J.K.Kim,[42] S.C.Kim,[42] W.W.Kinnison,[24] A.Kirkby,[32] D.Kirkby,[32] J.Kirkby,[17] D.Kiss,[14] W.Kittel,[31] A.Klimentov,[15,28] A.C.König,[31] A.Kopp,[47] I.Korolko,[28] V.Koutsenko,[15,28] R.W.Kraemer,[34] W.Krenz,[1] A.Kunin,[15,28] P.Lacentre,[47,♮,♯] P.Ladron de Guevara,[26] G.Landi,[16] C.Lapoint,[15] K.Lassila-Perini,[48] P.Laurikainen,[21] A.Lavorato,[38] M.Lebeau,[17] A.Lebedev,[15] P.Lebrun,[25] P.Lecomte,[48] P.Lecoq,[17] P.Le Coultre,[48] H.J.Lee,[8] C.Leggett,[3] J.M.Le Goff,[17] R.Leiste,[47] E.Leonardi,[36] P.Levtchenko,[37] C.Li,[20] C.H.Lin,[50] W.T.Lin,[50] F.L.Linde,[2,17] L.Lista,[29] Z.A.Liu,[7] W.Lohmann,[47] E.Longo,[36] W.Lu,[32] Y.S.Lu,[7] K.Lübelsmeyer,[1] C.Luci,[17,36] D.Luckey,[15] L.Luminari,[36] W.Lustermann,[48] W.G.Ma,[20] M.Maity,[10] G.Majumder,[10] L.Malgeri,[17] A.Malinin,[28] C.Maña,[26] D.Mangeol,[31] P.Marchesini,[48] G.Marian,[43,§] A.Marin,[11] J.P.Martin,[25] F.Marzano,[36] G.G.G.Massaro,[2] K.Mazumdar,[10] S.Mele,[17] L.Merola,[29] M.Meschini,[16] W.J.Metzger,[31] M.von der Mey,[1] Y.Mi,[22] D.Migani,[9] A.Mihul,[13] A.J.W.van Mil,[31] H.Milcent,[17] G.Mirabelli,[36] J.Mnich,[17] P.Molnar,[8] B.Monteleoni,[16] R.Moore,[3] T.Moulik,[10] R.Mount,[32] F.Muheim,[19] A.J.M.Muijs,[2] S.Nahn,[15] M.Napolitano,[29] F.Nessi-Tedaldi,[48] H.Newman,[32] T.Niessen,[1] A.Nippe,[22] A.Nisati,[36] H.Nowak,[47] Y.D.Oh,[42] G.Organtini,[36] R.Ostonen,[21] S.Palit,[12] C.Palomares,[26] D.Pandoulas,[1] S.Paoletti,[36] P.Paolucci,[29] H.K.Park,[34] I.H.Park,[42] G.Pascale,[36] G.Passaleva,[17] S.Patricelli,[29] T.Paul,[12] M.Pauluzzi,[33] C.Paus,[17] F.Pauss,[48] D.Peach,[17] Y.J.Pei,[1] S.Pensotti,[27] D.Perret-Gallix,[4] B.Petersen,[31] S.Petrak,[8] A.Pevsner,[5] D.Piccolo,[29] M.Pieri,[16] P.A.Piroué,[35] E.Pistolesi,[27] V.Plyaskin,[28] M.Pohl,[48] V.Pojidaev,[28,16] H.Postema,[15] J.Pothier,[17] N.Produit,[19] D.Prokofiev,[37] J.Quartieri,[38] G.Rahal-Callot,[48] N.Raja,[10] P.G.Rancoita,[27] M.Rattaggi,[27] G.Raven,[39] P.Razis,[30] D.Ren,[48] M.Rescigno,[36] S.Reucroft,[12] T.van Rhee,[44] S.Riemann,[47] K.Riles,[3] O.Rind,[3] A.Robohm,[48] J.Rodin,[43] B.P.Roe,[3] L.Romero,[26] S.Rosier-Lees,[4] Ph.Rosselet,[22] S.Roth,[1] J.A.Rubio,[17] D.Ruschmeier,[8] H.Rykaczewski,[48] J.Salicio,[17] E.Sanchez,[26] M.P.Sanders,[31] M.E.Sarakinos,[21] G.Sauvage,[4] C.Schäfer,[1] V.Schegelsky,[37] S.Schmidt-Kaerst,[1] D.Schmitz,[1] M.Schneegans,[4] N.Scholz,[48] H.Schopper,[49] D.J.Schotanus,[31] J.Schwenke,[1] G.Schwering,[1] C.Sciacca,[29] D.Sciarrino,[19] L.Servoli,[33] S.Shevchenko,[32] N.Shivarov,[41] V.Shoutko,[28] J.Shukla,[24] E.Shumilov,[28] A.Shvorob,[32] T.Siedenburg,[1] D.Son,[42] V.Soulimov,[29] B.Smith,[15] P.Spillantini,[16] M.Steuer,[15] D.P.Stickland,[35] H.Stone,[35] B.Stoyanov,[41] A.Straessner,[1] K.Sudhakar,[10] G.Sultanov,[18] L.Z.Sun,[20] G.F.Susinno,[19] H.Suter,[48] J.D.Swain,[18] X.W.Tang,[7] L.Tauscher,[6] L.Taylor,[12] Samuel C.C.Ting,[15] S.M.Ting,[15] S.C.Tonwar,[10] J.Tóth,[14] C.Tully,[35] K.L.Tung,[7] Y.Uchida,[15] J.Ulbricht,[48] E.Valente,[36] G.Vesztergombi,[14] I.Vetlitsky,[28] G.Viertel,[48] M.Vivargent,[4] S.Vlachos,[6] H.Vogel,[34] H.Vogt,[47] I.Vorobiev,[17,28] A.A.Vorobyov,[37] A.Vorvolakos,[30] M.Wadhwa,[6] W.Wallraff,[1] J.C.Wang,[15] X.L.Wang,[20] Z.M.Wang,[20] A.Weber,[1] S.X.Wu,[15] S.Wynhoff,[1] J.Xu,[11] Z.Z.Xu,[20] B.Z.Yang,[20] C.G.Yang,[7] H.J.Yang,[7] M.Yang,[7] J.B.Ye,[20] S.C.Yeh,[51] J.M.You,[34] An.Zalite,[37] Yu.Zalite,[37] P.Zemp,[48] Y.Zeng,[1] Z.P.Zhang,[20] B.Zhou,[11] Y.Zhou,[3] G.Y.Zhu,[7] R.Y.Zhu,[32] A.Zichichi,[9,17,18] F.Ziegler,[47] G.Zilizi.[43,§]

1 I. Physikalisches Institut, RWTH, D-52056 Aachen, FRG[§]
III. Physikalisches Institut, RWTH, D-52056 Aachen, FRG[§]
2 National Institute for High Energy Physics, NIKHEF, and University of Amsterdam, NL-1009 DB Amsterdam, The Netherlands
3 University of Michigan, Ann Arbor, MI 48109, USA
4 Laboratoire d'Annecy-le-Vieux de Physique des Particules, LAPP,IN2P3-CNRS, BP 110, F-74941 Annecy-le-Vieux CEDEX, France
5 Johns Hopkins University, Baltimore, MD 21218, USA
6 Institute of Physics, University of Basel, CH-4056 Basel, Switzerland
7 Institute of High Energy Physics, IHEP, 100039 Beijing, China[△]
8 Humboldt University, D-10099 Berlin, FRG[§]
9 University of Bologna and INFN-Sezione di Bologna, I-40126 Bologna, Italy
10 Tata Institute of Fundamental Research, Bombay 400 005, India
11 Boston University, Boston, MA 02215, USA
12 Northeastern University, Boston, MA 02115, USA
13 Institute of Atomic Physics and University of Bucharest, R-76900 Bucharest, Romania
14 Central Research Institute for Physics of the Hungarian Academy of Sciences, H-1525 Budapest 114, Hungary[‡]
15 Massachusetts Institute of Technology, Cambridge, MA 02139, USA
16 INFN Sezione di Firenze and University of Florence, I-50125 Florence, Italy
17 European Laboratory for Particle Physics, CERN, CH-1211 Geneva 23, Switzerland
18 World Laboratory, FBLJA Project, CH-1211 Geneva 23, Switzerland
19 University of Geneva, CH-1211 Geneva 4, Switzerland
20 Chinese University of Science and Technology, USTC, Hefei, Anhui 230 029, China[△]
21 SEFT, Research Institute for High Energy Physics, P.O. Box 9, SF-00014 Helsinki, Finland
22 University of Lausanne, CH-1015 Lausanne, Switzerland
23 INFN-Sezione di Lecce and Universitá Degli Studi di Lecce, I-73100 Lecce, Italy
24 Los Alamos National Laboratory, Los Alamos, NM 87544, USA
25 Institut de Physique Nucléaire de Lyon, IN2P3-CNRS,Université Claude Bernard, F-69622 Villeurbanne, France
26 Centro de Investigaciones Energeticas, Medioambientales y Tecnologicas, CIEMAT, E-28040 Madrid, Spain♭
27 INFN-Sezione di Milano, I-20133 Milan, Italy
28 Institute of Theoretical and Experimental Physics, ITEP, Moscow, Russia
29 INFN-Sezione di Napoli and University of Naples, I-80125 Naples, Italy
30 Department of Natural Sciences, University of Cyprus, Nicosia, Cyprus
31 University of Nijmegen and NIKHEF, NL-6525 ED Nijmegen, The Netherlands
32 California Institute of Technology, Pasadena, CA 91125, USA
33 INFN-Sezione di Perugia and Universitá Degli Studi di Perugia, I-06100 Perugia, Italy
34 Carnegie Mellon University, Pittsburgh, PA 15213, USA
35 Princeton University, Princeton, NJ 08544, USA
36 INFN-Sezione di Roma and University of Rome, "La Sapienza", I-00185 Rome, Italy
37 Nuclear Physics Institute, St. Petersburg, Russia
38 University and INFN, Salerno, I-84100 Salerno, Italy
39 University of California, San Diego, CA 92093, USA
40 Dept. de Fisica de Particulas Elementales, Univ. de Santiago, E-15706 Santiago de Compostela, Spain
41 Bulgarian Academy of Sciences, Central Lab. of Mechatronics and Instrumentation, BU-1113 Sofia, Bulgaria
42 Center for High Energy Physics, Adv. Inst. of Sciences and Technology, 305-701 Taejon, Republic of Korea
43 University of Alabama, Tuscaloosa, AL 35486, USA
44 Utrecht University and NIKHEF, NL-3584 CB Utrecht, The Netherlands
45 Purdue University, West Lafayette, IN 47907, USA
46 Paul Scherrer Institut, PSI, CH-5232 Villigen, Switzerland
47 DESY-Institut für Hochenergiephysik, D-15738 Zeuthen, FRG
48 Eidgenössische Technische Hochschule, ETH Zürich, CH-8093 Zürich, Switzerland
49 University of Hamburg, D-22761 Hamburg, FRG
50 National Central University, Chung-Li, Taiwan, China
51 Department of Physics, National Tsing Hua University, Taiwan, China
§ Supported by the German Bundesministerium für Bildung, Wissenschaft, Forschung und Technologie
‡ Supported by the Hungarian OTKA fund under contract numbers T019181, F023259 and T024011.
§ Also supported by the Hungarian OTKA fund under contract numbers T22238 and T026178.
♭ Supported also by the Comisión Interministerial de Ciencia y Technología.
♯ Also supported by CONICET and Universidad Nacional de La Plata, CC 67, 1900 La Plata, Argentina.
♮ Supported by Deutscher Akademischer Austauschdienst.
◇ Also supported by Panjab University, Chandigarh-160014, India.
△ Supported by the National Natural Science Foundation of China.

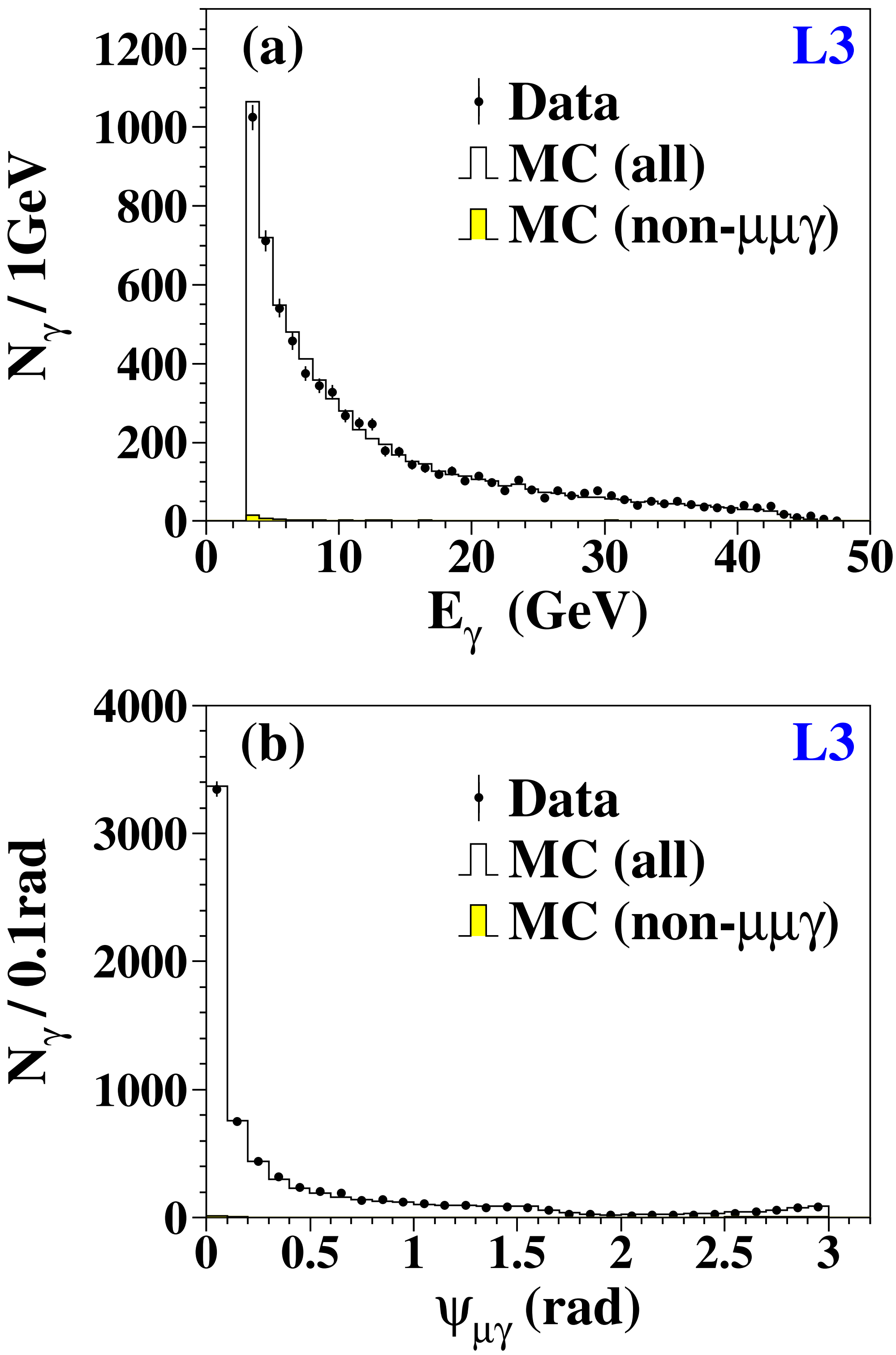

Figure 1: The number N_γ of photon candidates in the $e^+e^- \rightarrow \mu^+\mu^-\gamma$ sample as a function of (a) photon energy E_γ and (b) the angle $\psi_{\mu\gamma}$ of the photon to the closest muon. The points with error bars denote the data and the histograms denote the Monte Carlo predictions.

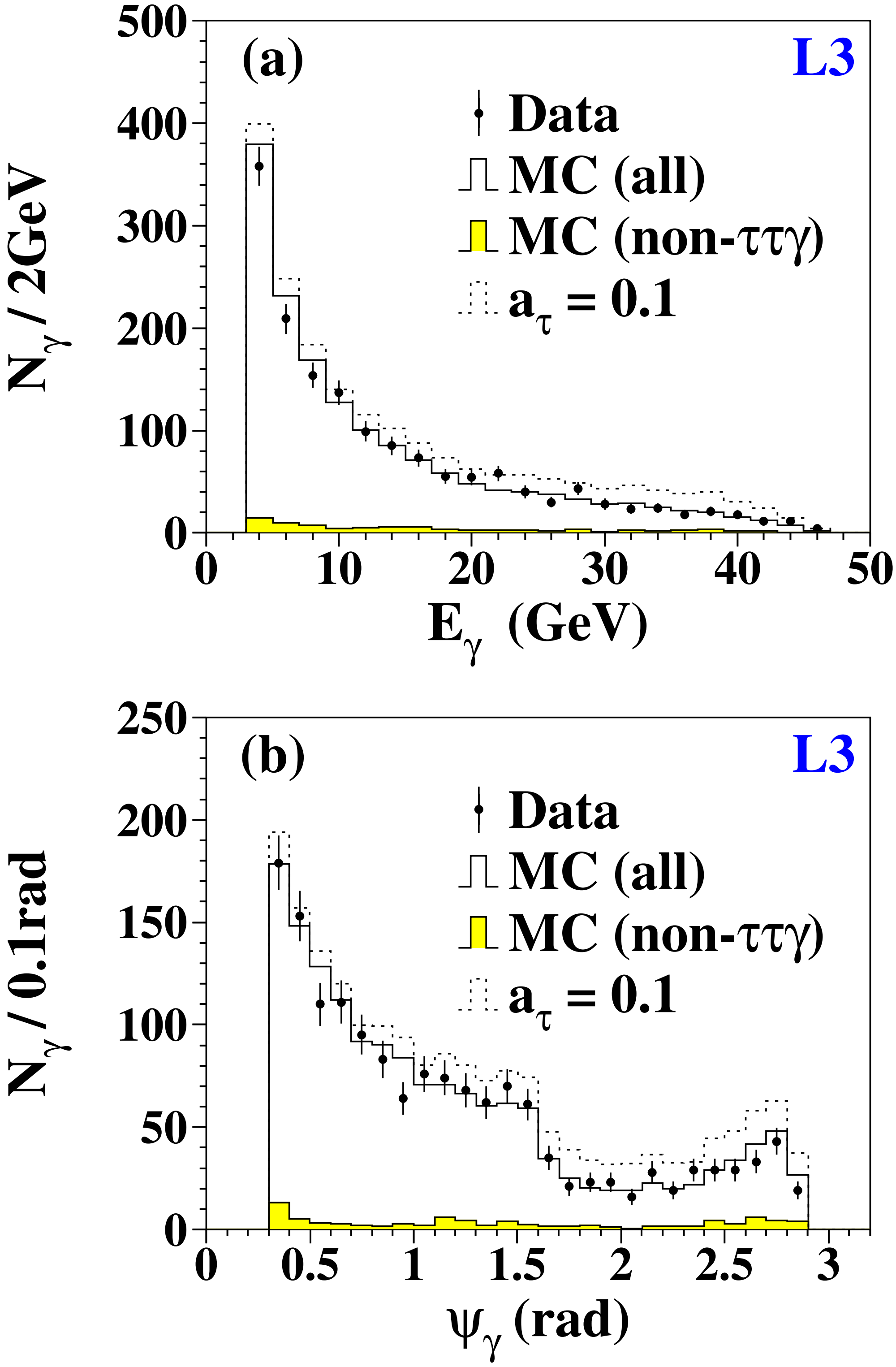

Figure 2: The number N_γ of photon candidates in the $e^+e^- \to \tau^+\tau^-\gamma$ sample as a function of (a) photon energy E_γ and (b) the isolation angle ψ_γ defined in the text. The points with error bars denote the data and the solid histograms denote the Monte Carlo predictions, assuming the SM values of a_τ and d_τ. For illustration, the dashed histograms show how the distributions would appear for $a_\tau = 0.1$. Both the increase in the total cross section and the relatively greater importance of photons with large E_γ and ψ_γ are evident.

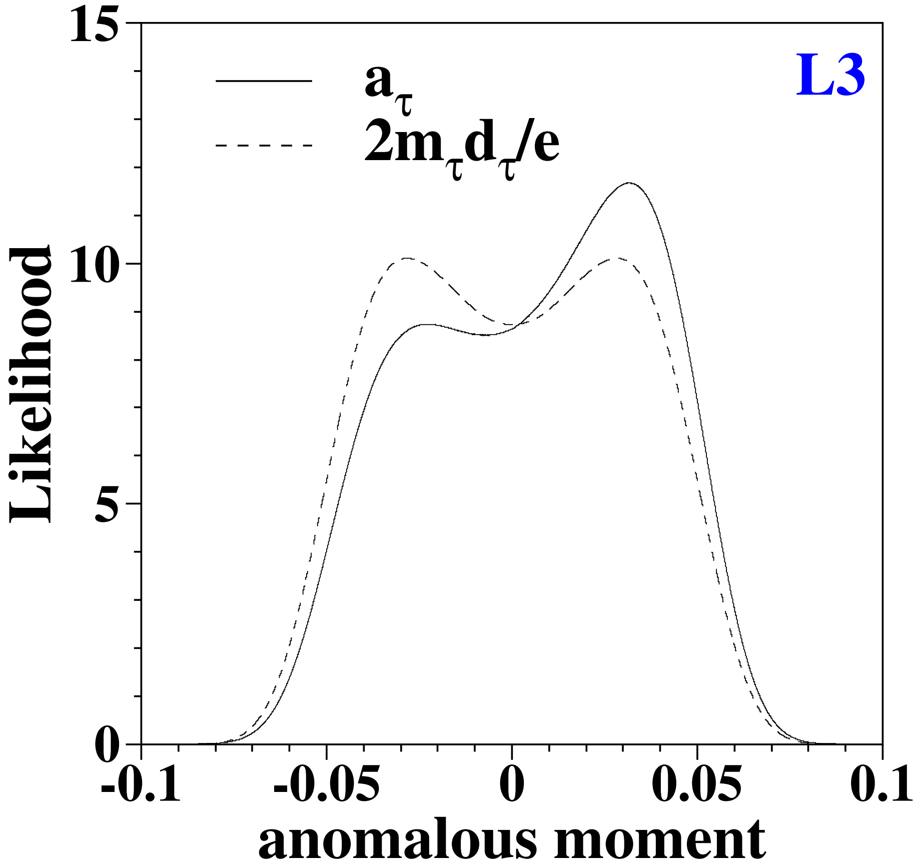

Figure 3: The likelihoods for data and Monte Carlo samples to agree as a function of the anomalous moments, a_τ (solid line) and $2m_\tau d_\tau/e$ (dashed line). The effects of systematic uncertainties are included.